Electronic Supplementary Material (ESI) for Nanoscale.

SUPPLEMENTARY INFORMATION

Nanotopography Regulates Motor Neuron Differentiation of Human Pluripotent Stem Cells

Weiqiang Chen,*[a,b] Shuo Han,[a] Weyi Qain,[b] Shinuo Weng,[a] Haiou Yang,[a,c] Yubing Sun,[a] Luis G. Villa-Diaz,[d] Paul H. Krebsbach,[e] and Jianping Fu*[a,f,g]

[a]Department of Mechanical Engineering, University of Michigan, Ann Arbor, MI 48105, USA; [b]Department of Mechanical and Aerospace Engineering, New York University, New York, NY 10012, USA; [c]Shanghai Children's Medical Center, Shanghai Jiao Tong University, Shanghai, 200062, China; [d]Department of Biological Sciences, Oakland University, Rochester, MI 48105, USA; [e]School of Dentistry, University of California Los Angeles, Los Angeles, CA 90095, USA; [f]Department of Biomedical Engineering, University of Michigan, Ann Arbor, MI 48105, USA; [g]Department of Cell and Developmental Biology, University of Michigan Medical School, Ann Arbor, MI 48109, USA.

*Correspondence should be addressed to W. Chen (email: wchen@nyu.edu) or J. Fu (email: jpfu@umich.edu).

Supplementary Figures 1 to 12

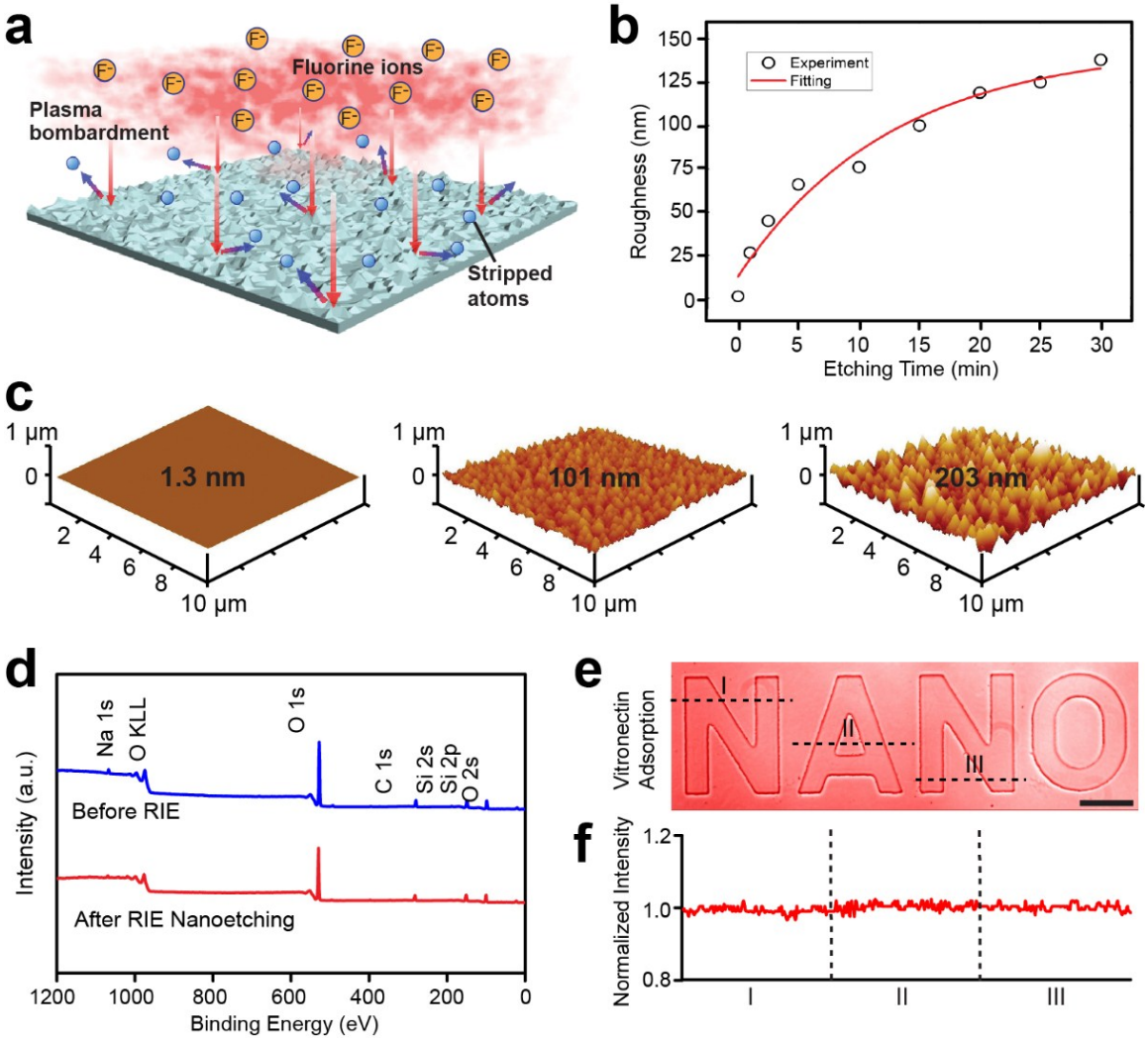

Fig. S1. Characterization of nanoengineered nanotopographic surfaces. (**a**) Schematic of nanotopography generated by RIE on glass surfaces. (**b**) Nanoroughness as a function of RIE process time. (**c**) AFM topographs of glass substrates before (*left*; R_q = 1.3 nm) and after (*middle*&*right*; R_q = 101 nm & 203 nm) RIE processing. (**d**) XPS survey spectra measured for glass substrates before (*blue* curve) and after RIE nanoetching (*red* curve). (**e**) Merged phase-contrast and anti-vitronectin immunofluorescence image of micropatterned glass substrate with vitronectin coating. (**f**) Normalized fluorescence intensity at the dash lines (I-III) in e. No significant difference in fluorescence intensity of the adsorbed vitronectin proteins was observed in the unprocessed smooth and RIE-processed nanorough regions.

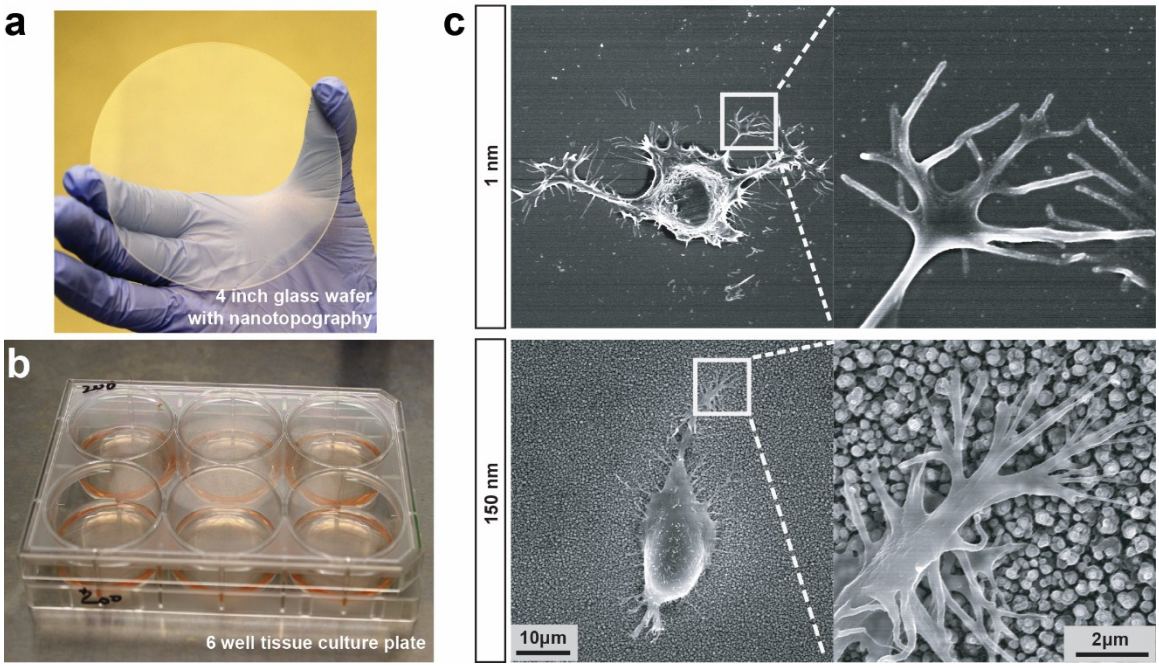

Fig. S2. (**a&b**) Photograph showing a 4-inch glass wafer with nanotopographic features (**a**) before cut and placed into tissue culture dishes (**b**). (**c**) Representative SEM images showing hPSCs plated on smooth (R_q = 1 nm) and nanorough (R_q = 150 nm) glass surfaces.

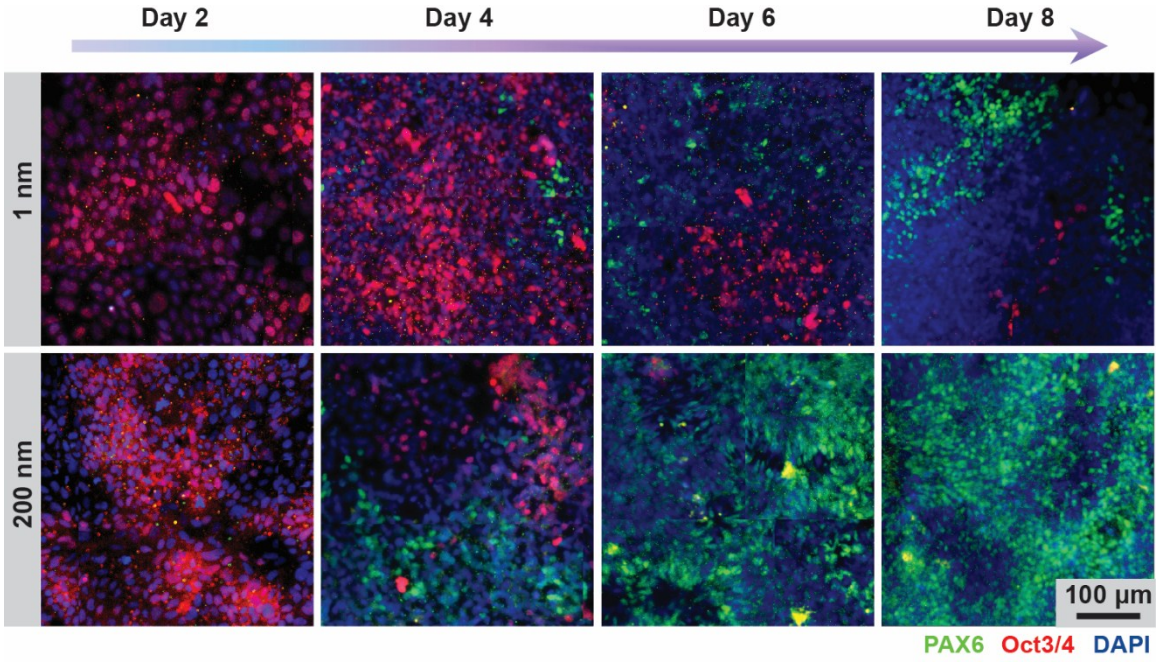

Fig. S3. Representative immunofluorescence images showing temporal expression of pluripotency (Oct3/4; red) and neuroectodermal (PAX6; green) markers during neural induction of hPSCs in neural induction medium on smooth (top; R_q = 1 nm) and nanorough (bottom; R_q = 200 nm) glass substrates as indicated.

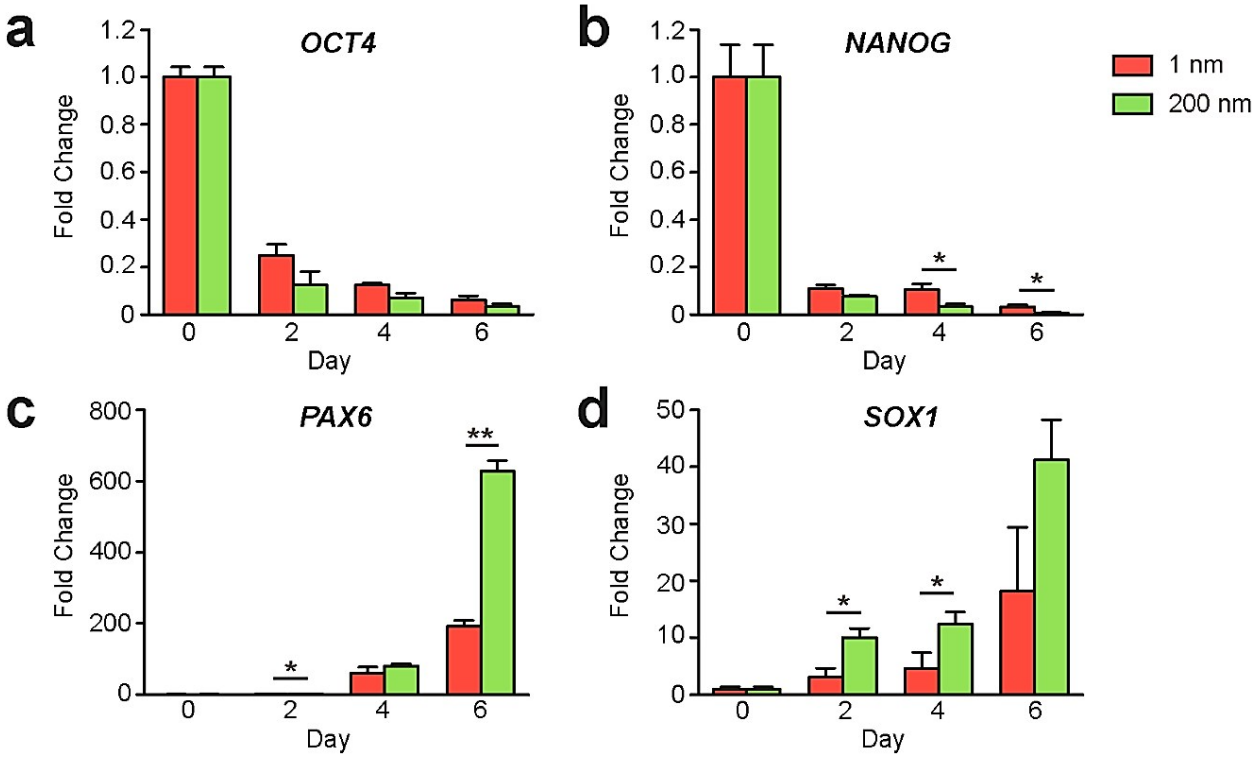

Fig. S4. qRT-PCR analysis for temporal expression of pluripotency (*OCT4* and *NANOG*; **a&b**) and neuroectodermal (*PAX6* and *SOX1*; **c&d**) markers during neural induction of hPSCs. hPSCs were cultured in neural induction medium on smooth (R_q = 1 nm) and nanorough (R_q = 200 nm) surfaces. Expression level of *OCT4*, a pluripotency marker, was reduced on both nanorough and smooth glass substrates at day 2. *NANOG,* another gene associated with pluripotency, decreased more significantly at both day 4 and 6 on nanorough (R_q = 200 nm) glass substrates compared with smooth controls (R_q = 1 nm). Genes associated with neural lineages, including *PAX6* and *SOX1*, showed greater levels of expression on nanorough surfaces after day 2 when compared to smooth controls. Expression level of each gene was normalized to data from undifferentiated hPSCs. Data represent the mean ± s.e.m with n = 3. P-values were calculated using the Student's paired sample t-test. *, $P < 0.05$; **, $P < 0.01$.

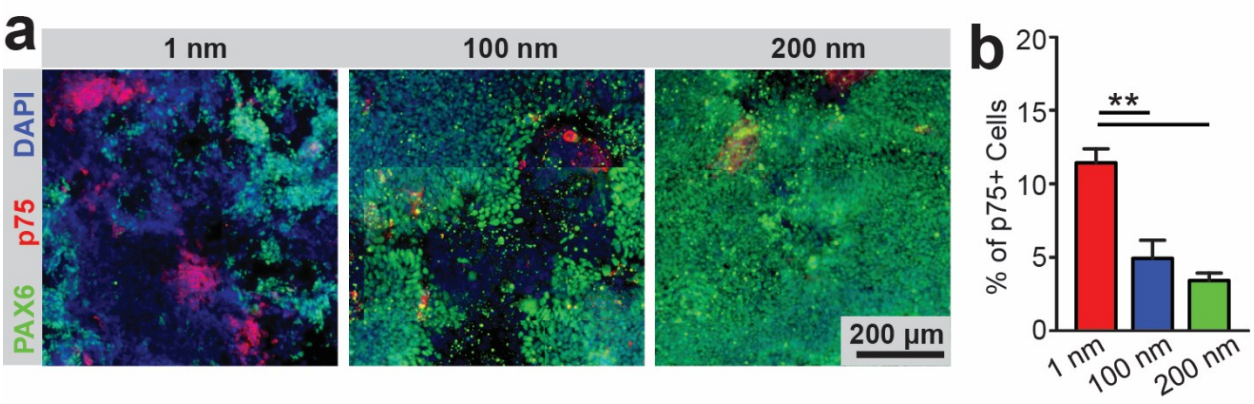

Fig. S5. (**a**) Representative immunofluorescence images showing PAX6+ NEs and p75+ NCs after 8 days of culture on smooth (R_q = 1 nm) and nanorough (R_q = 100 nm & 200 nm) glass surfaces. (**b**) Percentages of p75+ NC cells derived from hPSCs at day 8 as a function of nanoroughness. Data represent the mean ± s.e.m. with n = 3. P-values were calculated using the Student's paired sample t-test. **, $P < 0.01$.

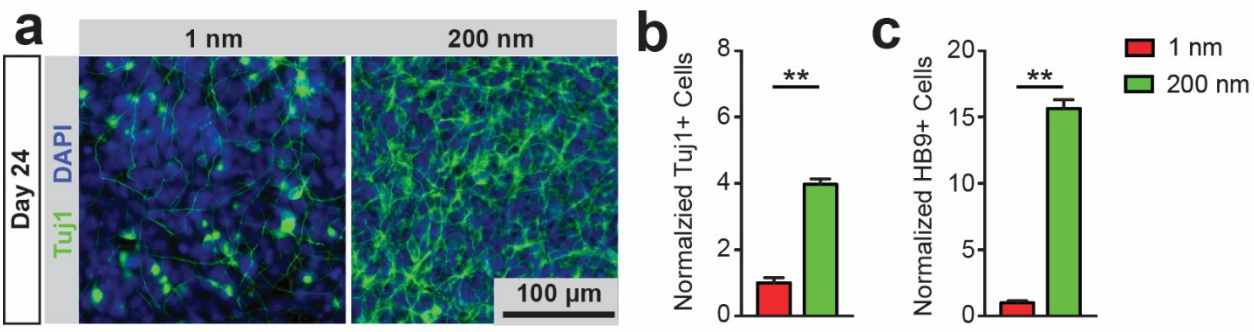

Fig. S6. (**a**) Representative immunofluorescence images showing Tuj1+ cells after 24 days of differentiation in MN differentiation medium on smooth (R_q = 1 nm) and nanorough (R_q = 200 nm) glass substrates. (**b-c**) Bar plots showing normalized Tuj1+ (b) and HB9+ (c) cell numbers at day 24 as a function of surface nanoroughness as indicated.

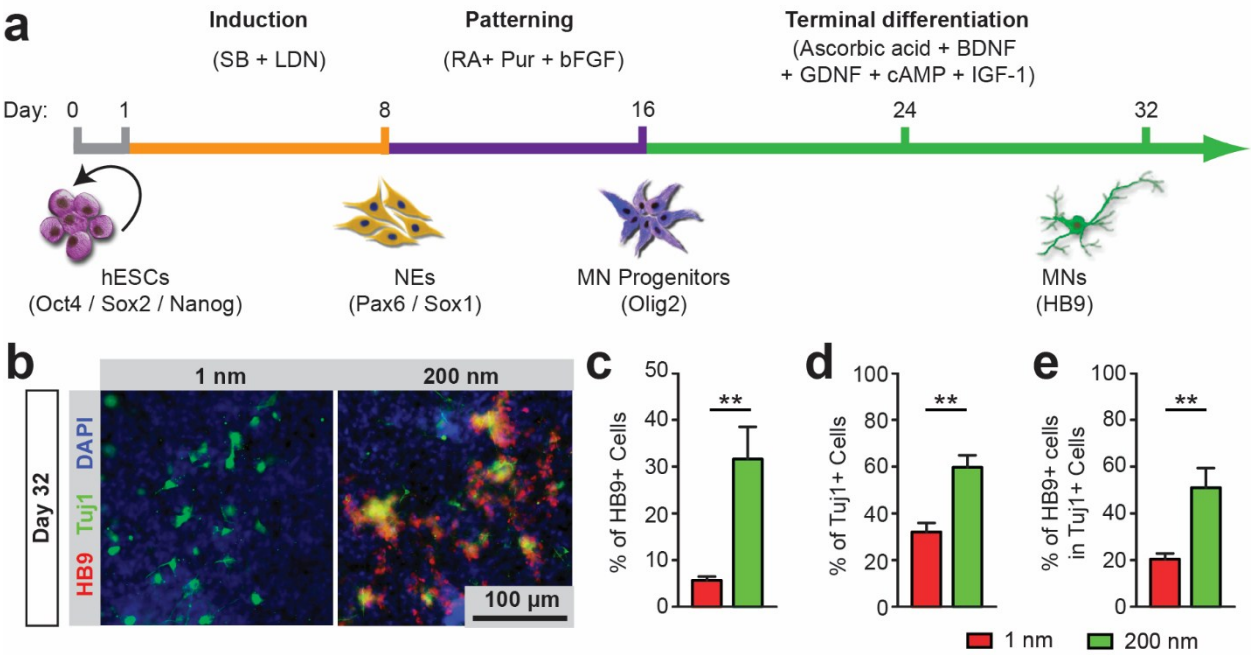

Fig. S7. Purity and yield of motor neurons (MNs) derived from hPSCs are improved on nanorough substrates with a 32-day differentiation protocol. (**a**) Schematic diagram showing experimental design for sequential neural induction, patterning, and maturation of MNs from hPSCs. hPSCs were cultured on vitronectin-coated smooth (R_q = 1 nm) and nanorough (R_q = 200 nm) glass substrates in neural induction medium containing the dual Smad inhibitors SB and LDN for 8 days and then in MN differentiation medium containing purmorphamine (Pur), basic fibroblast growth factor (bFGF) and retinoic acid (RA) for an additional 8 days. Putative MN progenitor cells collected at day 16 were transferred onto coverslips and cultured in MN maturation medium containing brain-derived neurotrophic factor (BDNF), ascorbic acid, cyclic adenosine monophosphate (cAMP) and insulin-like growth factor 1 (IGF-1) for another 16 days. (**b**) Representative immunofluorescence images showing Tuj1+ and HB9+ cells at day 32. (**c-e**) Bar plots showing percentages of HB9+ (**c**) and Tuj1+ (**d**) cells and percentages of HB9+ cells in Tuj1+ cells (**e**) at day 32. Data represent the mean ± s.e.m. with n = 3. P-values were calculated using the Student's paired sample t-test. **, $P < 0.01$.

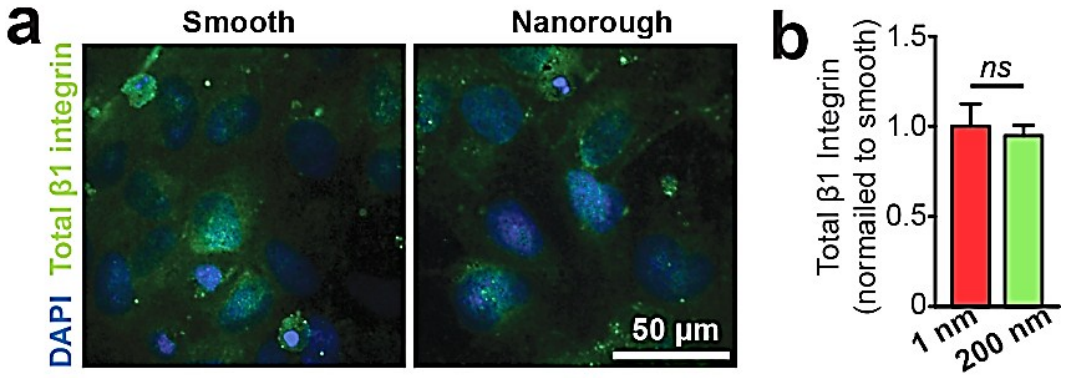

Fig. S8. (**a**) Immunofluorescence images showing total β1 integrin in undifferentiated hPSCs on smooth (R_q = 1 nm) and nanorough (R_q = 200 nm) glass substrates after 48 hr of culture. (**b**) Bar graphs showing quantitative results of normalized total β1 integrin for Oct3/4+ hPSCs cultured on substrates with different nanoroughness as indicated. Error bars represent ± s.e.m. with n = 10. P-values were calculated using the Student's paired sample t-test. *ns*, $P > 0.05$.

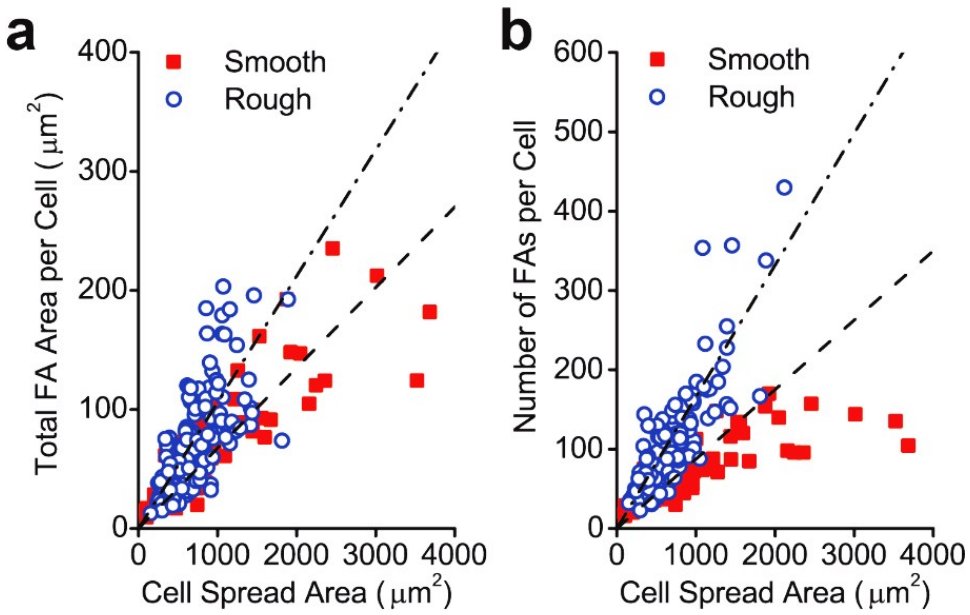

Fig. S9. Subcellular analysis of focal adhesion (FA) in hPSCs cultured on smooth (R_q = 1 nm) and nanorough (R_q = 200 nm) glass substrates.

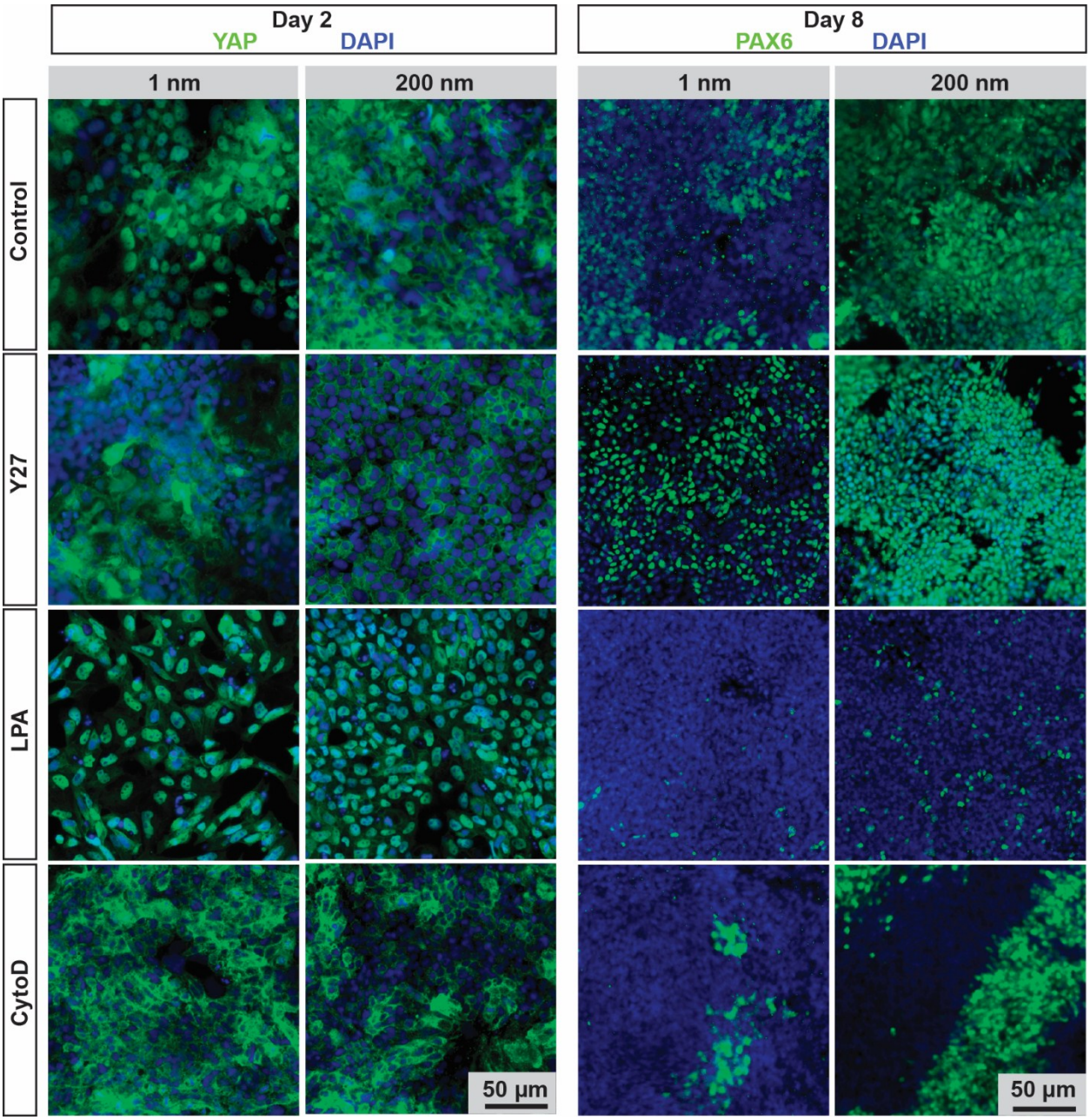

Fig. S10. Representative immunofluorescence images showing nanoroughness-dependent subcellular localization of YAP in hPSCs at day 2 and PAX6+ NEs derived from hPSCs at day 8 on smooth (R_q = 1 nm) and nanorough (R_q = 200 nm) glass surfaces under different drug treatments as indicated.

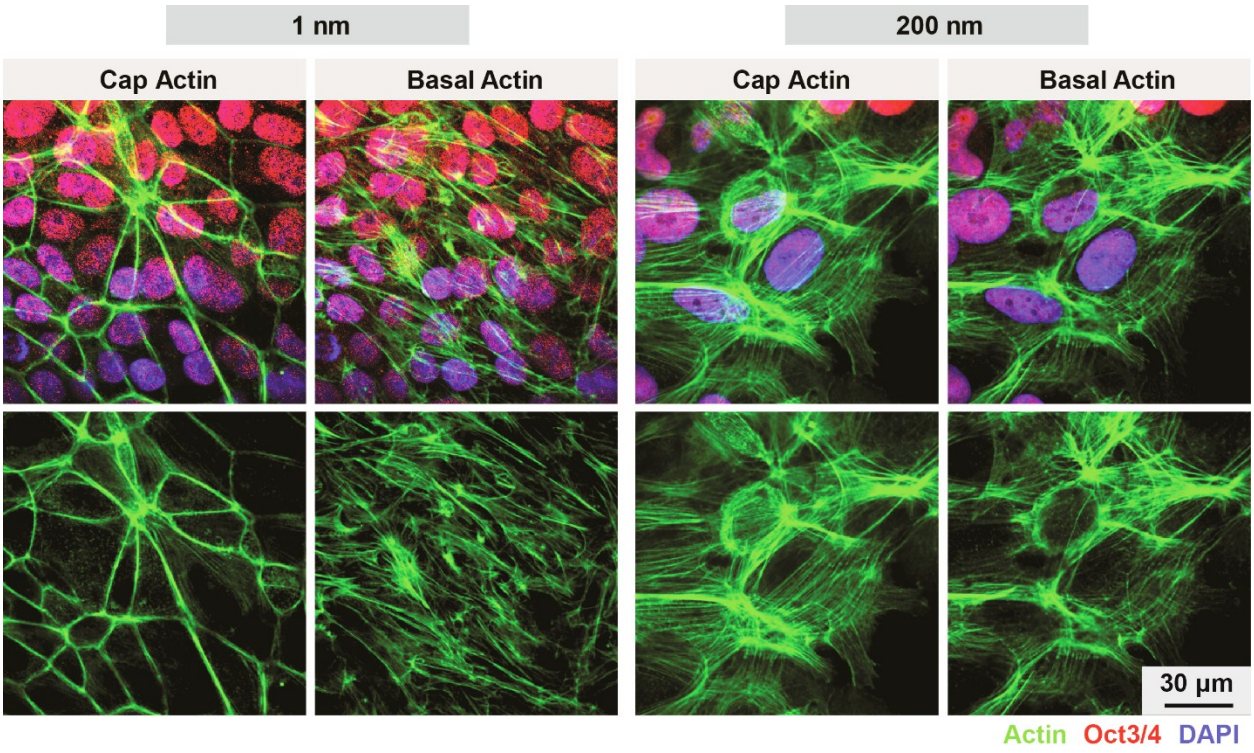

Fig. S11. Immunofluorescence images showing actin CSK (green), including cap actin (left panels) and basal actin (right panels) filament organization, in Oct3/4+ hPSCs cultured on smooth (R_q = 1 nm) and nanorough (R_q = 200 nm) glass substrates as indicated. The confocal microscopy sections show the actin filament network at the apical surface (cap actin) and basal surface (basal actin) of Oct3/4+ hPSCs cultured on smooth (R_q = 1 nm) and nanorough (R_q = 200 nm) glass substrates. There are thick, parallel, and highly contractile perinuclear cap actin filament bundles observed in the hPSCs on the nanorough substrates, while well-developed basal stress fibers were found and apical perinuclear actin cap is absence in hPSCs on the smooth substrates.

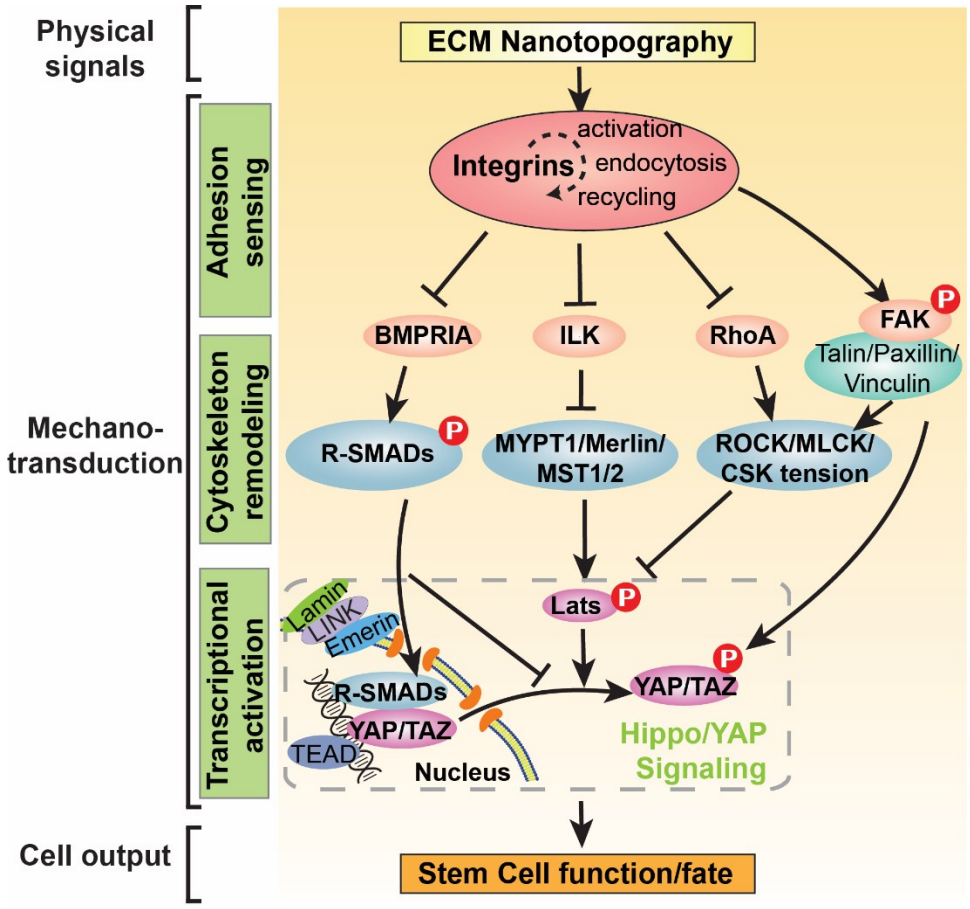

Fig. S12. Nanotopography-triggered signaling controls hPSC behaviors.